Desalination and Water Treatment
www.deswater.com
doi: 10.1080/19443994.2016.1164082

57 (2016) 26114–26129
November

Taylor & Francis
Taylor & Francis Group

Facile and economic one-pot synthesis of rigid functional-polyurethane for the effective treatment of heavy metal-contaminated urban storm water run-off

Mohsen Vafaeifard[a], Gooyong Lee[a], Shatirah Akib[a], Shaliza Ibrahim[a,*], Yeomin Yoon[b], Min Jang[a,c,*]

[a] *Faculty of Engineering, Department of Civil Engineering, University of Malaya, Kuala Lumpur 50603, Malaysia, emails: mohsen.vafaeifard@gmail.com (M. Vafaeifard), bluewater0703@gmail.com (G. Lee), s.mohamed_akib@hw.ac.uk (S. Akib), shaliza@um.edu.my (S. Ibrahim), Tel. +60 3 7967 7649, +82 2 940 5180; emails: minjang@um.edu.my, heejaejang@gmail.com, minjang@kw.ac.kr (M. Jang)*
[b] *Department of Civil and Environmental Engineering, University of South Carolina, Columbia, SC 29208, USA, email: yoony@cec.sc.edu*
[c] *Department of Environmental Engineering, Kwangwoon University, 447-1, Wolgye-Dong Nowon-Gu, Seoul, Korea*

Received 7 September 2015; Accepted 23 February 2016

ABSTRACT

In this study, highly permeable rigid polyurethanes (PU) incorporating calcium oxide (CaO) (PU/CaO) composite materials were prepared via a facile and economic one-pot synthesis method and characterized for remediation of heavy metal-contaminated urban storm water run-off (USR) in a fixed-bed column. Column tests were conducted to investigate various parameters, and data were interpreted using the Bed Depth Service Time model to predict service time. Among the media tested, 25% CaO-incorporated PU (PU/CaO-25) had the highest adsorption capacity of Cu(II). PU/CaO-25 had about 2.5-fold higher rigidity (0.38 MPa) than a "typical" rigid polymer (0.15 MPa). Hydraulic conductivity tests showed PU/CaO-25 (avg. 0.4 mm) had a permeability (0.108 cm s^{-1}) equivalent or higher than reference sands. Specific structural features of PU/CaO-25 and the remediation mechanism were also determined using FESEM/EDS, XRD, N_2 gas isotherm and chemical equilibrium modeling. Moreover, column tests using simulated USR showed that all heavy metals were removed by PU/CaO-25 to below their regulation levels at ~1,100 bed volumes. Based on the physicochemical properties and functionality, PU/CaO-25 may be useful as an effective filter material in USR treatment and reuse applications.

Keywords: Polyurethane; Urban storm water run-off; Adsorption; Heavy metals

1. Introduction

Nowadays, urban storm water run-off (USR) contaminated by heavy metals has significant negative impacts on receiving water. Flooding is also a "traditional" problem due to typically heavy rainfall in tropical countries, especially becoming an issue with urbanization. Protection of agricultural land, urban rivers, and streams from flooding in inhabited urban areas, especially with polluted water, are essential for USR management and treatment, as well as appropriately treated USRs can be used as a valuable source for drinking, cleaning, and farming purposes in urban area [1,2].

---

*Corresponding authors.

To address this issue, adsorption is a promising and suitable technique due to its simplicity, convenience, flexibility in design and ease of operation, low maintenance costs, and high efficiency [3–18]. Furthermore, as a great advantage of adsorption, a filtration system can be designed readily and established at any location with flooding. Thus, it especially requires that the filter media have high rigidness, removal capacities, and hydraulic conductivity (HC) at the same time. Recently, polymers have been investigated in removing heavy metals and have been explored in terms of treatment efficiency and removal mechanisms of heavy metals since they could be easily tailored for strength, pore structure, and functionalization [19–24].

In this study, we synthesized rigid polyurethane (PU) incorporating calcium oxide (CaO) (PU/CaO) composite materials via a facile, rapid, and economical one-pot synthesis route, and assessed its feasibility for removing heavy metals in a synthetic USR. As a widely practiced remediation method, alkaline materials have been applied to remove heavy metals via hydrolysis. Among alkaline materials, CaO is economically feasible because of its rapid reaction. However, when CaO is applied to remove heavy metals, its surface is susceptible to becoming covered by hydrolyzed colloids of heavy metals, so that CaO is not used fully and remained as a huge sludge. Hypothetically, when CaO is incorporated into PU, the armoring possibility could be reduced because CaO is located mainly in the PU framework and hydrolyzed heavy metal colloids could be separately deposited on PU surface. In addition, the addition of CaO could also increase the physical strength as filler.

The objectives of this study were to (1) examine the properties of the synthesized PU/CaO such as its rigidity and HC, (2) investigate the adsorption capability of PU/CaO for removing heavy metals in water using a fixed-bed column and the Bed Depth Service Time (BDST) model, and finally (3) investigate the specific structural features and remediation mechanism using FESEM/EDS, XRD, N_2 gas isotherm, and chemical equilibrium modeling. To our knowledge, this is the first reported study to develop a preparation method of functionalized polymer in an energy-efficient, massive producible, and cost-effective manner for the application of USR treatment.

2. Materials and methods

2.1. Materials

Stock solutions containing various heavy metals were prepared by dissolving the required amount of copper nitrate [$Cu(NO_3)_2$], lead nitrate [$Pb(NO_3)_2$], zinc sulfate [$Zn(SO_4)_2$], or nickel sulfate [$Ni(SO_4)_2$] in distilled (DI) water. Polyol ($C_2H_6O_2$) and MDI ($C_{15}H_{10}N_2O_2$) were purchased from Portal Trading, Penang, Malaysia. Powdered CaO with purity >99% was purchased from R&M Marketing, Essex, UK.

2.2. Preparation of PU and PU/CaO

The PU materials were made by exothermic reactions between polyol, having reactive hydroxyl (–OH) groups, and MDI, containing the isocyanate group (–NCO). To determine the optimum combination of precursors for PU, 13 samples prepared with different ratios of polyol and MDI were synthesized and measured for compressive strength and density. As a result, the maximum PU rigidity was achieved at a ratio of 1:2 (polyol/MDI). PU/CaO composites were prepared by adding predetermined amounts of CaO to the mixture of polyol and MDI. To investigate the effect of CaO, the amount of CaO was varied from 0 to 25% of total weight of polyol and MDI. In the synthesis method of composite, we designed 25% as the maximum of CaO incorporation since the mixing of all precursors was not homogeneous at >25%. The amounts of CaO were 0, 5, 10, 20, and 25% in PU, which corresponded to pure PU, PU/CaO-5, PU/CaO-10, PU/CaO-20, and PU/CaO-25, respectively. First, 0, 2.5, 5.1, 10.2, or 12.8 g of CaO was hand-mixed with 17 g of polyol in paper cups for 1 min. Then, 34 g of MDI were added to the CaO and polyol mixture with stirring at 2,000 rpm for 20 s. The mixture was allowed to rise freely in the paper cup. Then, samples were kept at room temperature for 10 h after the cream time (the time from mixing to the initiation of foaming) and rise time (the time from mixing to full expansion of foaming). All PU/CaO composites were cut and ground. Then, they were sieved to collect 0.2–0.9-mm samples to be used for the column tests. Fig. 1 shows FESEM for PU/CaO-5, PU/CaO-10, PU/CaO-20, and PU/CaO-25, respectively.

2.3. Column setup and tests

The column tests were carried out with small-scale columns (1.6-cm (ID) × 4.5-cm (L)). Glass wool was used at the bottom and top of the column. The prepared PU/CaO was added to the column and DI water was pumped into the column to remove loose particles of CaO. Then, a solution containing heavy metals was flowed into the column using a peristaltic pump at the designed flow rate, and samples at the outlet were obtained at various bed volumes (BVs). To avoid hydrolysis and precipitation of heavy metals

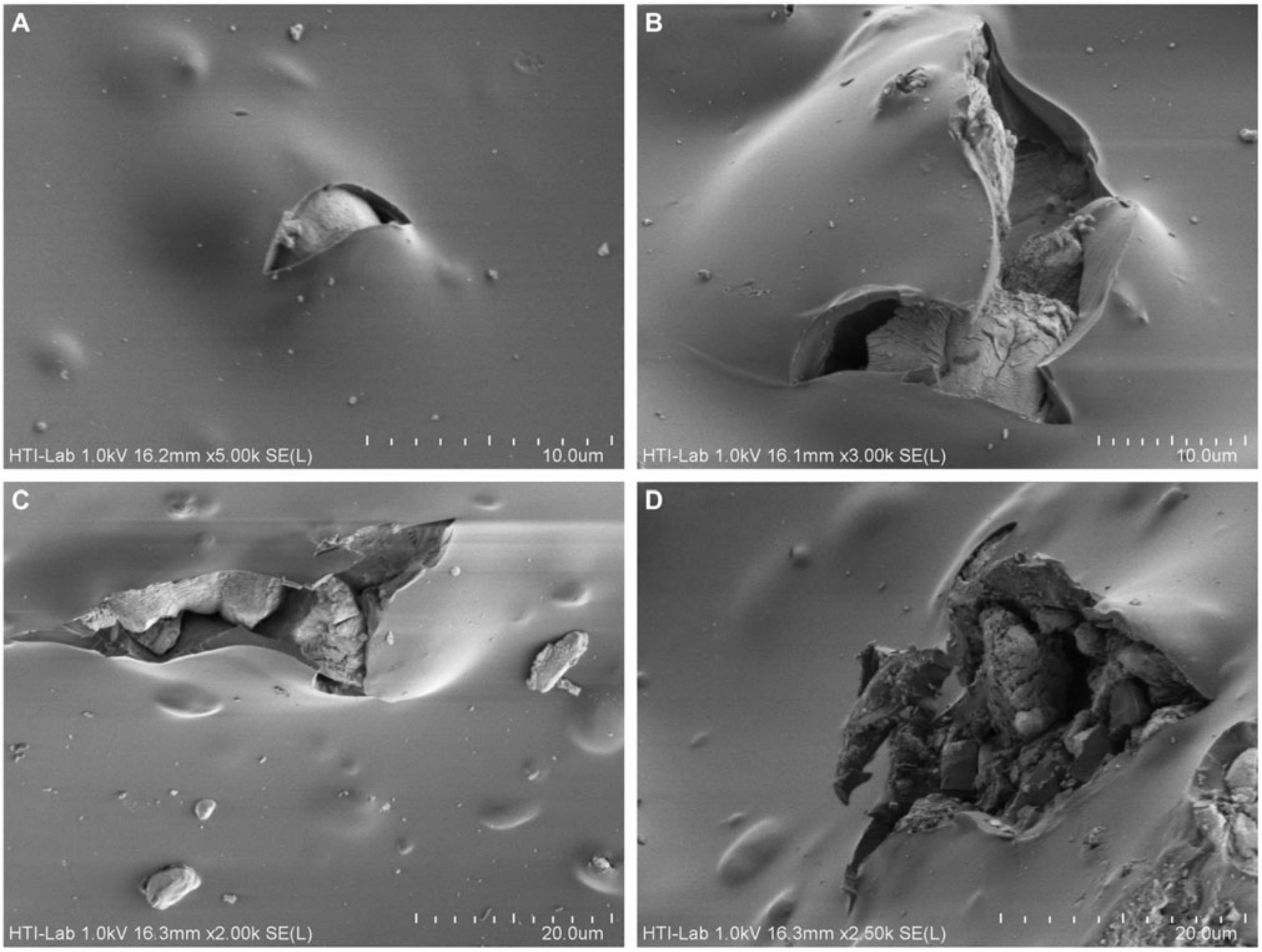

Fig. 1. FESEM images of (A) PU/CaO-5, (B) PU/CaO-10, (C) PU/CaO-20, and (D) PU/CaO-25.

due to high pH, the pH of the inlet water was adjusted to 4.0. Stock solutions of Cu(II), Ni(II), Zn(II), and Pb(II) at 0.31, 0.54, and 1 mmol L^{-1} were prepared using DI water, at which the ionic strength was adjusted to 0.1 M using sodium chloride (NaCl). The column was run using an upflow mode to remove any channeling effect [25]. The pH was measured at the column outlet. Continuous-flow column tests were conducted to assess the effects of important parameters such as CaO content, bed height, flow rate, concentration, and type of heavy metals.

2.4. Column tests using synthetic USR

Synthetic USR containing Cu(II), Zn(II), and Pb(II) was prepared using tap water. In this study, we selected actual USR data in Singapore because its precipitation and urbanization are similar to Malaysia where few data are available. The reported concentration ranges for Cu(II), Zn(II), and Pb(II) were 44.8–241, 436.4–1,127, and 52.3–90.3 μg L^{-1}, respectively [26]. Two columns were packed with 2.0 g of PU/CaO-25 (4.5-cm bed height). Column tests were run at 0.5 and 1.2 mL min^{-1} flow rates to assess the effect of residence time (i.e. slow and fast conditions of USR) for the removal of heavy metals. Both columns were fed with synthetic USR with 320, 820, and 130 μg L^{-1} of Cu(II), Zn(II), and Pb(II), respectively. Table 1 shows the water quality of simulated USR in water. The operational pH was 6.9 while hardness and sulfate were 38 mg L^{-1} (as $CaCO_3$) and 10 mg L^{-1}, respectively [27]. In the tap water, other heavy metals, such as Al(III), Fe(III), and Ni(II), were also detected, at concentrations of 141, 298, and 30 μg L^{-1}, respectively.

Table 1
Water quality of simulated USR

Parameters	Values
pH	6.9
Copper	90 (μg L^{-1})
Zinc	259 (μg L^{-1})
Lead	95 (μg L^{-1})
Calcium	13,430 (μg L^{-1})
Magnesium	1073 (μg L^{-1})
Manganese	28 (μg L^{-1})
Iron	298 (μg L^{-1})
Cadmium	20 (μg L^{-1})
Sodium	12,250 (μg L^{-1})
Aluminum	141 (μg L^{-1})
Nickel	30 (μg L^{-1})
Hardness	38 (mg $CaCO_3$ L^{-1})
Sulfate	10 (mg L^{-1})

3. Results and discussion

3.1. Effect of CaO on the PU matrix

PU media incorporating various amounts of CaO (0, 5, 10, 20, and 25%) were prepared and used to fill columns to a 4.5-cm height. Column tests were performed to investigate the effect of CaO amount incorporated into PU for removing Cu(II) from water. The Cu(II) solution (65 mg L^{-1} or 1 mmol L^{-1}) was passed through the columns with a flow rate of 2.5 mL min^{-1}. Fig. 2(A) shows the outlet concentrations of Cu(II) for 800 BVs. Cu(II) removal increased as the CaO amount increased, from 0 to 25%. PU/CaO-20, −15, −5, and pure PU removed dissolved Cu(II) up to 5, 4, 2, and 1 BVs, respectively. The Cu(II) concentration in the outlet increased sharply and 50% BT occurred at 9, 7, 4, and 2 BVs. However, PU/CaO-25 showed a higher removal capacity than the other media. For example, Cu(II) was completely removed by PU/CaO-25 until 8 BVs and increased slowly; 50% BT occurred after passing 116 BVs. The pH profiles were also measured during the column tests for all media and are presented in Fig. 2(B). The pure PU increased the pH from 4.0 to 7.0 for 5–6 BVs followed by a dramatic decrease to 4.5. However, PU/CaO-5, −10, −20, and −25 showed pH increases to 8.7, 10.5, 10.8, and 11.1, and then the pH decreased gradually to 5, 6.1, 6.2, and 6.5 at 200 BVs, respectively. Thus, the CaO incorporated in the PU had a major effect in raising the pH.

The accumulation removal capacities (ARCs) of Cu (II) for all media were calculated using the BT curve (Fig. 2(C)). The ARC was calculated using the following equation:

$$\mathrm{ARC} = QA = Q\int_{t=0}^{t=t_e} C_{\mathrm{Ad}}\,dt \quad (1)$$

where ARC (mg g^{-1}) can be calculated by multiplying flow rate (Q, L min^{-1}) and area (A) under the BT curve that can be obtained by integrating the adsorbed Cu(II) concentration (C_{Ad}, mg L^{-1}) at each time t (min). C_{Ad} can be calculated by subtracting the outlet concentration of Cu(II) from the inlet Cu(II) concentration (C_0).

Fig. 2(D) shows the ARCs according to the contents of CaO. Cu(II) uptake did not increase linearly with the increase in CaO, and PU/CaO-25 had a considerably higher ARC (0.94 mmol g^{-1}) than PU/CaO-20 (0.47 mmol g^{-1}) at 800 BV. Given these results, we suggest that the occupation site of CaO in the PU matrix may differ. In the case of 25% CaO incorporation, the higher amount of CaO may be more exposed at the surface and contact the solution, while at lower percentages CaO may exist predominantly within the frameworks of PU. Because PU/CaO-25 showed the highest removal efficiency, it was used in subsequent experiments.

3.2. Effect of flow rate

The effect of flow rate was studied with 0.5, 1.2, and 2.5 mL min^{-1}. The flow rate ranged from 3.6 to 18 min of empty bed contract time (EBCT), with which USR treatment can be properly simulated. The inlet concentrations of Cu(II) and bed height were maintained at 1 mmol L^{-1} and 4.5 cm, respectively. The breakthrough (BT) profiles are presented in Fig. 3(A). The breakthrough point (BTP) decreased slightly, from 102 to 97 BVs, as the flow rate increased from 0.5 to 1.2 mL min^{-1}. When the flow rate increased to 2.5 mL min^{-1}, Cu(II) increased immediately at the outlet and BTP was shortened significantly, to 9 BVs. Since the solute in the solution should have a sufficient time to penetrate and react with OH^-, a longer BTP could be obtained with a lower flow rate [28,29]. The ARCs of Cu(II) by PU/CaO-25 were 0.61 and 0.28 mmol g^{-1} for 0.5–2.5 mL min^{-1}, respectively, at 300 BVs. In more detail, when the flow rate decreased, N_0 and K_a increased, from 4,091 to 8,640 mg L^{-1} and 0.27 to 0.31 L mg^{-1} h^{-1}, respectively (Table 2). Subsequent experiments were conducted at 1.2 mL min^{-1} (EBCT, 7.5 min), which was selected as the optimum flow rate.

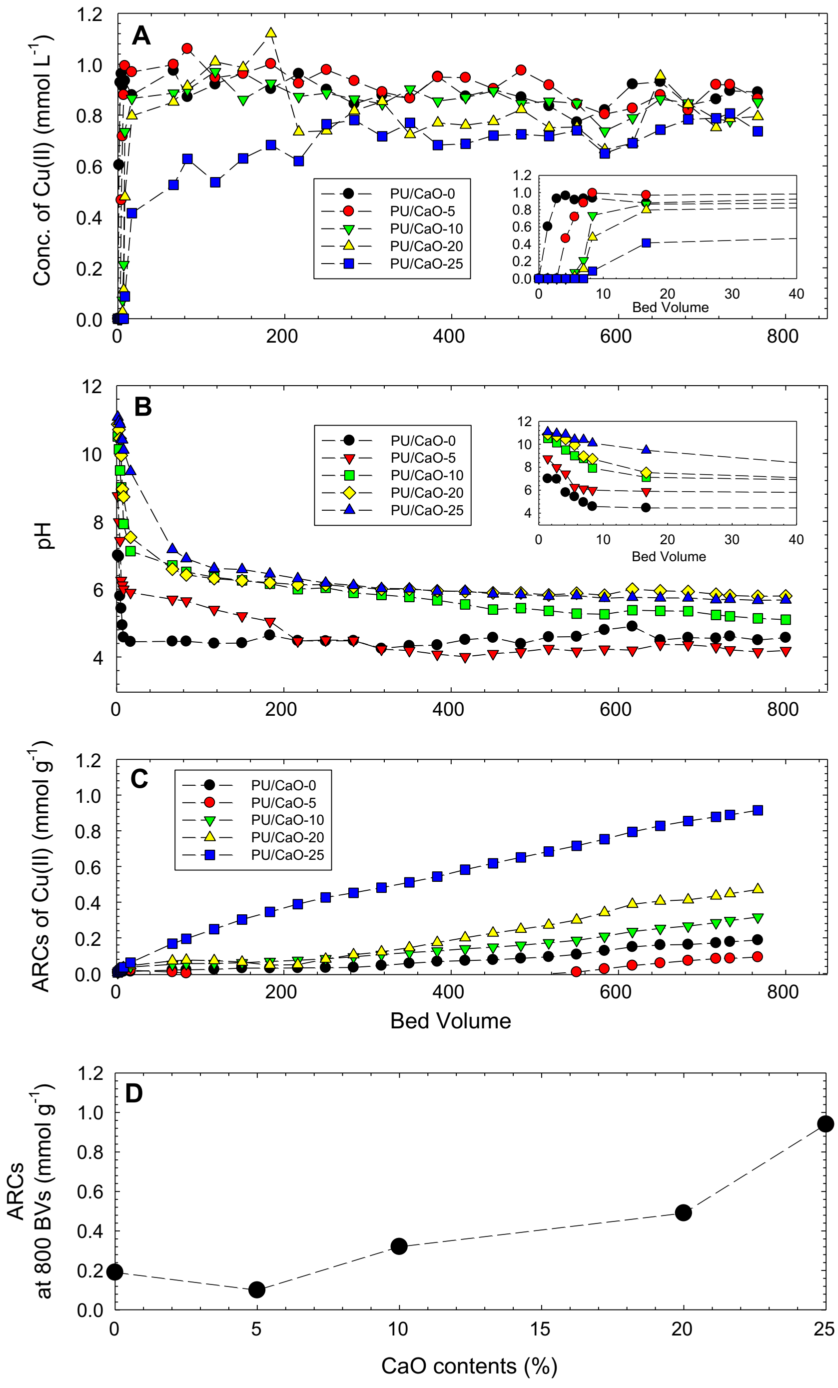

Fig. 2. (A) Effect of PU media incorporated by various amounts of CaO, (B) pH changes in outlet, (C) accumulated removal capacities of Cu(II), and (D) accumulated removal capacities (ARCs) at 800 BVs with CaO contents. (Flow rate = 2.5 mL min^{-1} and Cu(II) concentration = 0.9 mmol L^{-1}).

3.3. *Effect of heavy metal concentrations*

The effects of the influent concentration of metals (0.31, 0.54, or 1 mmol L^{-1}) on the removal of Cu(II) by PU/CaO-25 were assessed under the conditions of a 4.5-cm bed height and a 1.2 mL min^{-1} flow rate (Fig. 3(B)); the modeling parameters are presented in Table 2. PU/CaO-25 became saturated at different time and BTPs of Cu(II) removal were observed at

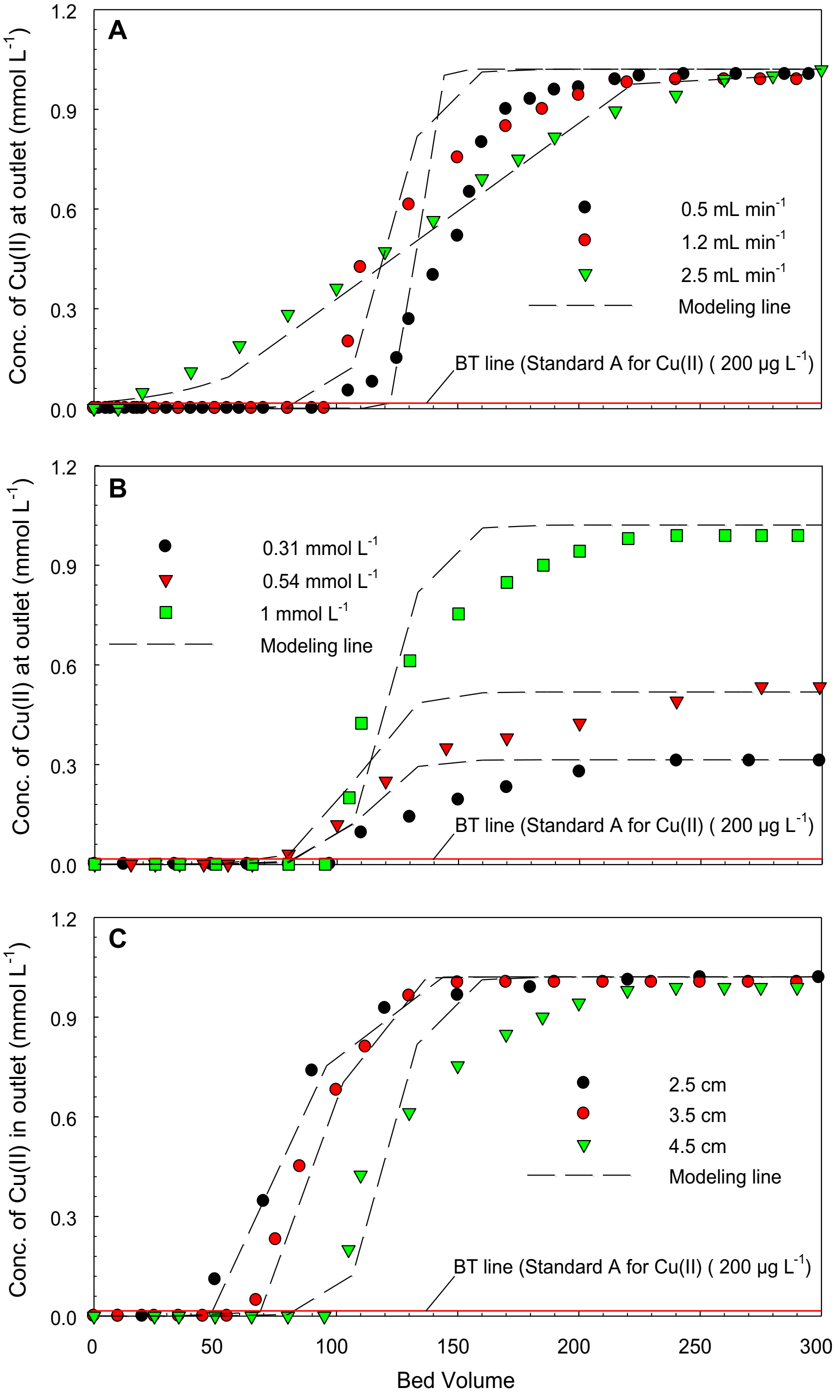

Fig. 3. Effect of (A) bed height, (B) inlet concentration, and (C) flow-rate on Cu(II) removal by PU/CaO-25.

107, 65, and 97 BVs for 0.31, 0.54, and 1 mmol L^{-1}, respectively. Therefore, there is no linear relationship between Cu(II) concentration and BTPs. And, the current results seem to show the concentration is independent to BTP. Accordingly, it can be assured that PU/CaO composite has a different removal mechanism of general sorption and precipitation which are mostly dependent on the heavy metal concentration. For example, a regular CaO-based precipitation and adsorption has a removal limitation by armoring effect and sorption site reduction. Especially, for the case of adsorption principle, BTPs can be

Table 2
Bed Depth Service Time (BDST) parameters for heavy metals removal by PU/CaO-25

Metals	Flowrate (mL min^{-1})	Conc.		Bed height (cm)	Slope (m_x) (min cm^{-1})	K_a (L mg^{-1} h^{-1})	N_0 (mg L^{-1})	RT (Sec)	q_0		R^2	BTP (BV)
		mmol L^{-1}	mg L^{-1}						mg g^{-1}	mmol g^{-1}		
Cu(II)	0.5	1	65	4.5	–2,933	0.31	8,640	1,080	38.8	0.61	0.99	102
	1.2				–3,542	0.30	7,914.2	450	35.6	0.60	0.99	97
	2.5				–3,355	0.27	4,091.0	216	18.40	0.28	0.92	9
Cu(II)	1.2	1	65	4.5	–3,542	0.30	7,914.2	450	35.6	0.60	0.99	97
		0.54	35		–4,314	0.42	3,531.6	450	15.8	0.24	0.98	65
		0.31	20		–3,803	0.79	2,202.7	450	9.9	0.15	0.99	107
Cu(II)	1.2	1	65	2.5	–1,680	0.54	5,759.7	250	22.1	0.34	0.96	25
				3.5	–2,303	0.40	6,315.5	350	26.0	0.40	0.97	52
				4.5	–3542	0.30	7,914.2	450	35.6	0.60	0.99	97
Cu(II)	1.2	1	65	4.5	–3,542	0.30	7,914.2	450	35.6	0.60	0.99	97
Ni(II)		1.1			–4,706	0.19	5,940.5	450	26.7	0.45	0.96	36
Zn(II)		0.99			–2,466	0.37	3,226.1	450	14.5	0.22	0.80	25
Pb(II)		0.31			–2,169	0.42	4,397.4	450	19.7	0.09	0.86	66

expected to be shorten by an increase of Cu(II) concentration. The main reason for the insensitive property with concentration, as shown at the proposed hypothesis, might be the special structural feature, in which OH^- continuously releases to precipitate Cu(II) without any effect of surface armoring since CaO separately exists.

3.4. Effect of column bed height

Column tests of Cu(II) removal by PU/CaO-25 were conducted to assess the effect of bed height. To generate different bed heights, 1.3, 1.7, and 2.0 g of PU/CaO-25 were added to the column to prepare bed heights of 2.5, 3.5, and 4.5 cm, respectively. Column tests were conducted at a 1.2 mL min^{-1} constant flow rate and 1 mmol L^{-1} initial Cu(II) concentration. Fig. 3(C) shows that Cu(II) removal capacity was dependent on the amount of PU/CaO-25. When the bed height increased from 2.5 to 4.5 cm, BTPs (0.003 mmol L^{-1} or 0.2 mg L^{-1}) increased from 25 to 97 BVs. The increase in adsorption with greater bed depth was simply due to the increase in adsorbent mass, which provides more adsorption sites for metal ions [30]. Consequently, the diffusion of the metal ions into the sorbent and fluid residence time could increase as the bed height increased. Hence, the solute had sufficient time to diffuse into the entirety of the sorbent mass, treating more BVs in the solution [31]. By calculating the removal capacity of Cu(II) by BDST modeling, 2.5–3.5-cm bed heights showed 0.34–0.40 mmol g^{-1} at 300 BVs, respectively. The 4.5-cm bed height exhibited the highest removal capacity (0.60 mmol g^{-1}) and a longer column lifetime. K_a, N_0, and R^2 values are reported in Table 2.

3.5. Bed depth service time (BDST)

Fig. 4 shows the plot of service time at 0.0157 mmol L^{-1} BT vs. bed height (cm) at a flow rate of 1.2 mL min^{-1}. The plot was linear and the correlation coefficient ($R^2 = 0.9734$) indicated the validity of the BDST model for the present system. The value of K_a characterizes the rate of transfer from the fluid phase to the solid phase. Generally, if K_a is large, even a short bed will increase BTP, but as K_a decreases, a progressively longer bed is required to avoid a short BTP.

3.6. Interaction mechanism of metal removal by PU/CaO-25

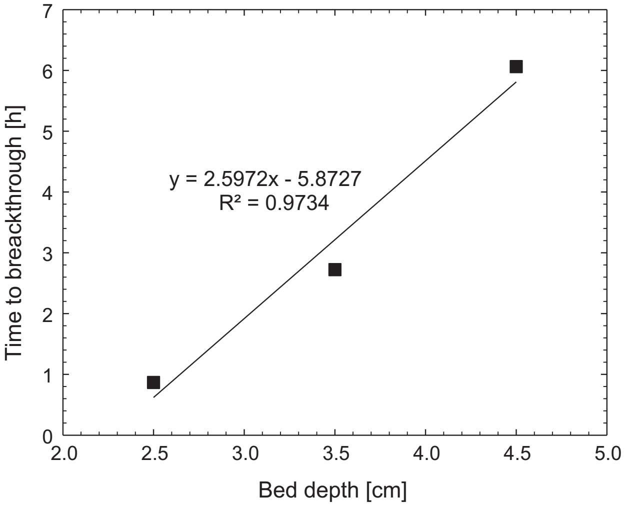

Fig. 4. A plot of time to BT according to bed depth at flow rate of 1.2 mL min^{-1}.

The BT curves for adsorption of Zn(II), Ni(II), Pb (II), and Cu(II) ions in the column are shown in Fig. 5. Column tests were conducted at a 1.2 mL min^{-1} constant flow rate and 65 mg L^{-1} initial concentration of each metal species at the column inlet. The removal data matched well with BDST modeling and showed a normal S-type sorption curve [32]. There are two domain mechanisms of metal removal by CaO: ion exchange and precipitation. At lower concentrations, ion exchange is dominant while precipitation is the main mechanism at higher concentrations [33]. Due to the alkaline situation, CaO has positively charged species, such as $CaOH_2^+$ or $CaOHCa^+$. Then, positively charged metals can be exchanged for the metal species. When the pH is low, however, H^+ ions compete with metal ions and are even released from the adsorbed species, resulting in a low removal capacity. Amarasinghe and Williams [34] reported that metal properties—such as mobility, ionic radius, and hydration enthalpy—can control metal adsorption. Metal ions with a lower radius have a higher probability of reacting with cationic surfaces by ion exchange. When the hydration radius of the metal ions is larger than the surface cations, ion exchange can be difficult. Since the radius of Cu(II) is the smallest of the metal ions tested, and even smaller than that of Ca(II) [35], Cu(II) ions can react with Ca(II) by ion exchange. However, because of their larger radii, Ni(II), Pb(II), and Zn(II) may have weak affinities for the active sorption sites. Based on the column results, adsorption capacities were in the order Cu(II) > Ni(II) > Pb(II) > Zn(II), while BTPs were in the order Cu(II) > Pb(II) > Ni(II) > Zn(II) (Table 2).

Metal precipitation occurs mainly with hydrolysis at higher pH values and concentrations [36]. In this study, selective precipitation was interpreted using the chemical equilibrium-modeling software, "Medusa."

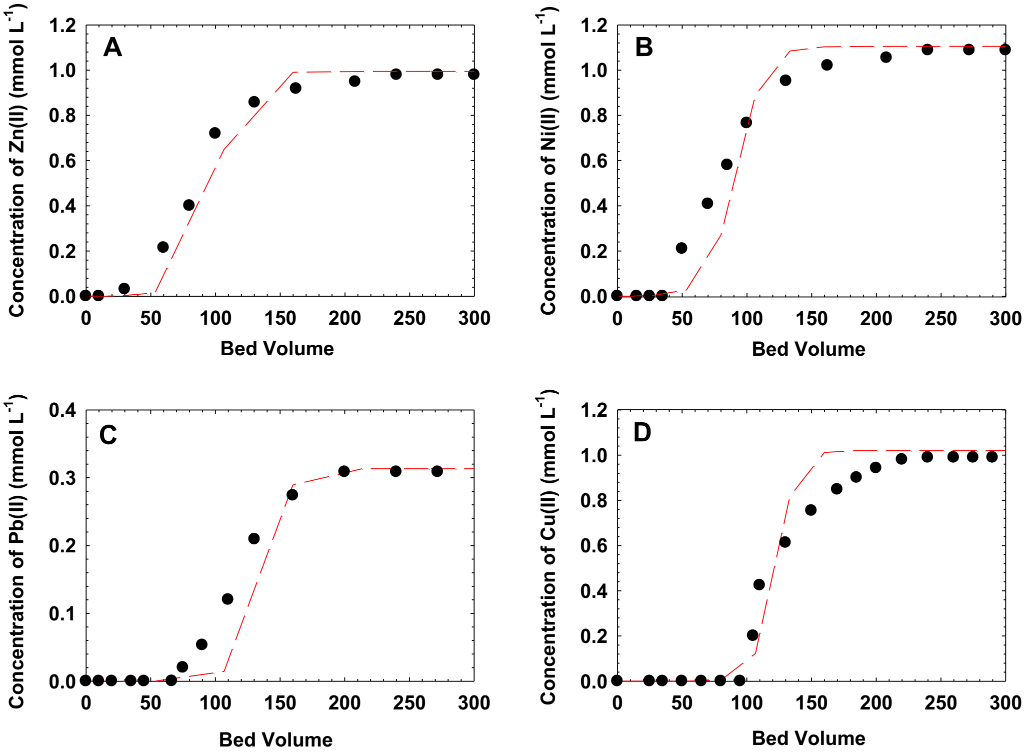

Fig. 5. Effect of type of heavy metals (A) Zn(II), (B) Ni(II), (C) Pb(II), and (D) Cu(II). Line (modeling) and dots (actuals data).

Using the software, it was found that CuO (cr), Pb$(OH)_2$ (c), $Ni(OH)_2$ (c), and ZnO (cr) existed dominantly as solid species at pH > 6.5, 7, 8, and 9, respectively. Because the outlet pH of all columns was in the range 7–8, metal precipitation would be expected to occur in the sequence Cu(II) > Pb(II) > Ni(II) > Zn(II), which is identical to that for BTPs. As shown at Section 3.3 (concentration effect), precipitation might be a dominant mechanism because metal concentration did not give a linear effect on BTPs.

3.6.1. FESEM/EDS

FESEM/EDS was used to evaluate the surface morphological changes of pure PU, PU/CaO-25, and Cu(II)-retained PU/CaO-25. Pure PU had a smooth surface without pores [20], while the surface was torn at the domain of CaO when 25% CaO was incorporated into the PU framework (Fig. 6(A) and (B). Fig. 6(C), (D), and (E) show the elemental mapping of C, O, and Ca, respectively, for PU/CaO-25, indicating that CaO existed mostly inside the framework of PU. Fig. 6(F) shows the EDS analysis of PU/CaO-25 and the existence of CaO on the surface of the PU. Fig. 6(G) and (H)–(K) show the morphology and elemental (C, O, Ca, and Cu) mapping of Cu(II)-retained PU/CaO-25. The major finding was that the locations of Ca(II) and Cu(II) were totally different. Ca(II) existed mostly under the surface while Cu(II) was on the surface, although not homogeneously distributed. At the stripped parts, Ca(II) was not detected, so the CaO may have dissolved out. Thus, it can be suggested that PU/CaO-25 provides an environment that facilitates retention of metal precipitates without occupying the surface of the CaO. The EDS analysis (Fig. 6(L)) revealed that Cu(II) was precipitated and present predominantly on the surface of the PU.

3.6.2. XRD

XRD was used to investigate the phase structures of the PU/CaO-25, and Cu(II)- and Zn(II)-retained PU/CaO-25 (Fig. 7). Sharp peaks at 64˚, 18˚, 48˚, and 51˚ were assigned to $Ca(OH)_2$ (JCPDS file 84–1264), indicating that CaO is hydrated during the synthesis of PU/CaO-25 and located mostly on the surface of the PU. Weak peaks at 29˚, 34˚, 54˚, and 63˚ were assigned to CaO (JCPDS file 77–2376) and were noticeable because CaO was covered by a PU framework. XRD analysis also confirmed that the precipitates of

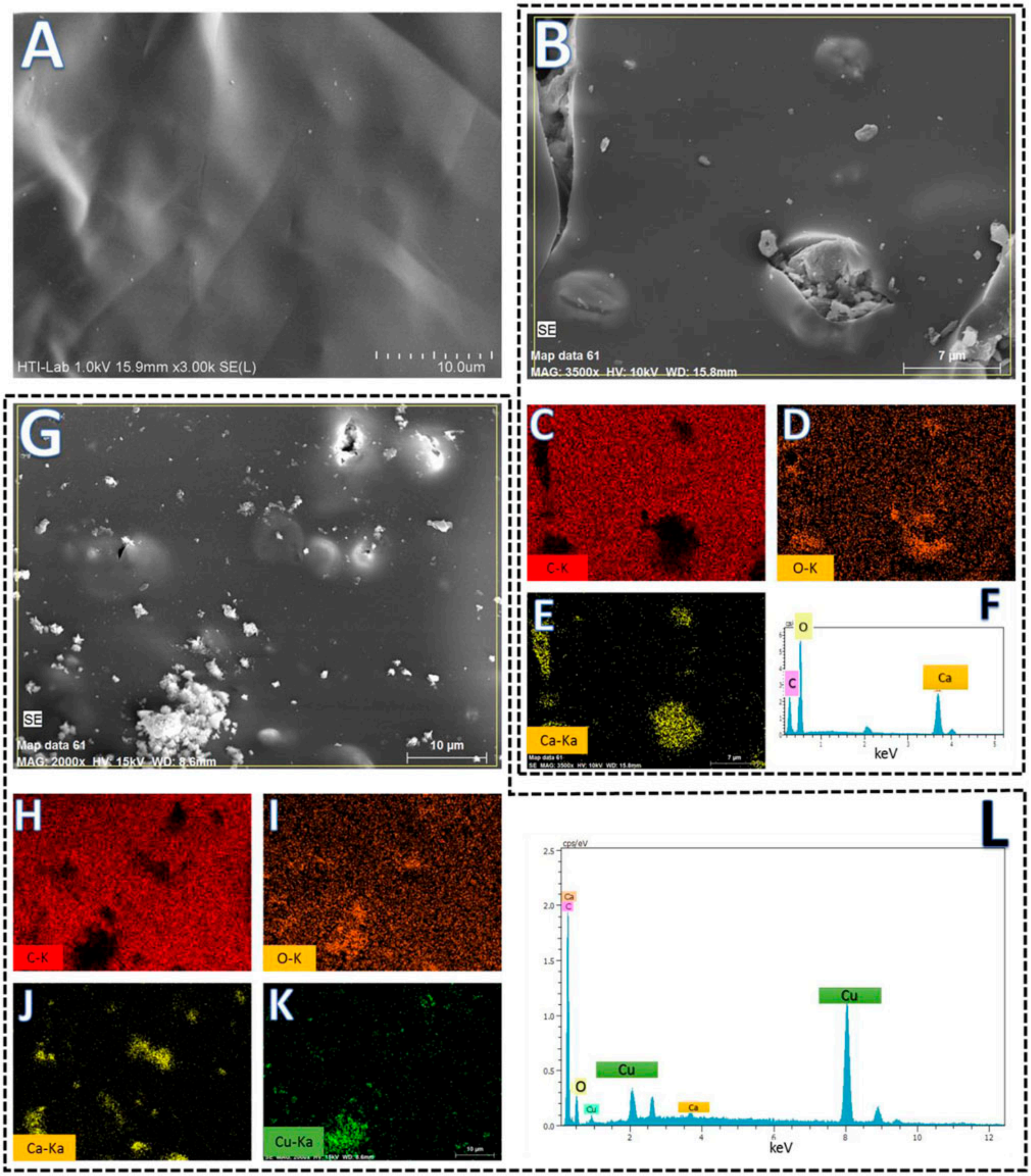

Fig. 6. FESEM images of (A) pure PU and (B) PU/CaO-25, elemental mapping of (C) C, (D) O, (E) Ca, (F) EDS for PU/CaO-25, (G) FESEM image of Cu(II) retained PU/CaO-25 [Cu(II) concentration, 1 mmol L^{-1}], elemental mapping of (H) C, (I) O, (J) Ca, (K) Cu, and (L) EDS for Cu(II) retained PU/CaO-25.

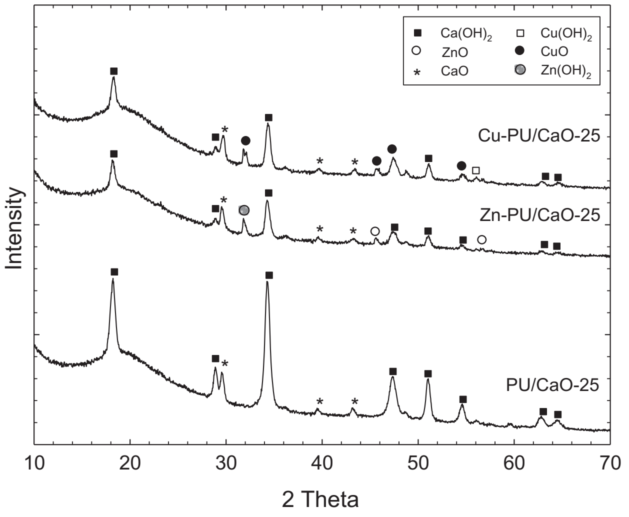

Fig. 7. XRD analysis of (A) PU/CaO–25, (B) Zn-PU/CaO–25, and (C) Cu-PU/CaO–25.

Zn(II) were ZnO (47°, 56°) and $Zn(OH)_2$ (33°), while those of Cu(II) were CuO (32°, 46°, 48°, 56°) and $Cu(OH)_2$ (57°). The intensities of the CaO peaks for PU/CaO-25 were similar to those for metal-retained PU/CaO-25, while the $Ca(OH)_2$ peaks were much reduced. From this result, we suggest that CaO was trapped in the framework of polymer and its hydrated form, $Ca(OH)_2$, mostly located at the surface, was used to remove Cu(II) or Zn(II). Thus, precipitation may be the dominant removal mechanism, as indicated by the results of column and modeling.

3.6.3. BET surface area

The BET surface areas of pure PU, PU/CaO-25 and Cu-PU/CaO-25 were 0.18, 1.0, and 0.92 $m^2\ g^{-1}$, while the pore volumes were 0.1×10^{-3}, 2.0×10^{-3}, and $2.9 \times 10^{-3}\ cm^3\ g^{-1}$, respectively. Thus, when CaO was incorporated at 25%, the surface area and pore volume increased by 5.5- and 20-fold, respectively. Thus, the addition of CaO created pore structures. Especially, according to the BJH desorption pore volume in Fig. 8, meso- (2–50 nm) and macropore structures (>50 nm) developed with the addition of CaO, whereas PU had no pores, as seen in the FESEM. Thus, these pore structures were created around CaO and become the channel for release of OH^- ions. In the case of Cu(II)-retained PU/CaO-25, the pore volume increased over a range of pore sizes because of inter-particle spaces of metal precipitates.

Table 3 shows the reported sorption capacities of Cu(II), Zn(II), Pb(II), and Ni(II) by various adsorbents in columns [12–14,16–18,37].

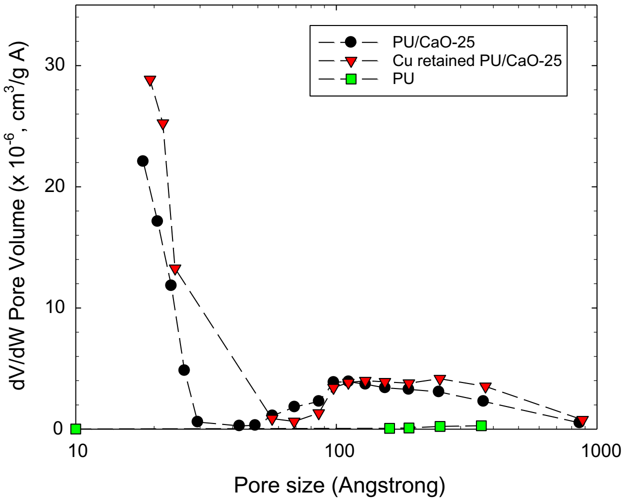

Fig. 8. BJH desorption pore volume according to pore size.

As observed, PU/CaO-25 possessed higher removal capacities for all metal species than the other listed adsorbents. It can be seen that PU-CaO has shorter HRT compared to all the adsorbents except manganese oxide coated zeolite [16] and modified clay [17]. Nevertheless, heavy metal removal capacity of PU-CaO composite is higher than other adsorbents. Although, comparison is difficult due to use of different concentrations and HRTs.

The higher removal capabilities with PU/CaO-25 may be due to its unique structural features. Armoring effect is one of the reasons that can reduce the removal capacity of adsorbents due to reducing the adsorbent reactivity by forming coverings on adsorbent surfaces and thereby reduced adsorption [38].

Based on the results of FESEM/EDS, N_2 gas isotherm, XRD, and chemical equilibrium modeling, we show schematics of PU, PU/CaO-25, and overall removal mechanisms for heavy metals (Fig. 9). CaO is the major reactive domain in PU/CaO-25, producing OH^- ions and could not be fully used if the surface of the CaO became armored by the hydrolyzed colloids of heavy metals. Thus, the PU surface supplies the sites for deposition of metal precipitates so that armoring does not occur; instead, OH^- is effectively and successively released through pores created by CaO to precipitate heavy metals in the liquid phase.

3.7. Compressive strength and hydraulic conductivity

Compressive stress-strain measurements showed 0.28–0.38 MPa for pure PU and PU/CaO-25, respectively. The form densities of PU and PU/CaO-25 were 55 and 75 $kg\ m^{-3}$, respectively. Typical rigid PU form

Table 3
Comparison of adsorption capacities, inlet concentrations, and hydraulic retention time (HRT) between PU/CaO-25 and references

Adsorbents	Heavy metals	q_0 (mg g^{-1})	Conc. (mg L^{-1})	HRT (Sec)	Refs.
Mucor rouxii	Pb(II)	4.06	10	1,800	[13]
Zeolite		1.67	5	440	[12]
ICZ		2.28	5	440	
PVA-MKC		6.30	150	990	[14]
PVA-MKC (Na$^+$ impregnated)		10.4	300	1,031	
PVA-MKC (Ca^{2+} impregnated)		9.98	300	1,031	
PU/CaO-25		19.7	65	450	This study
Sodium hydroxide-modified oil palm	Zn(II)	0.016	100	1,080	[15]
Zeolite		1.19	5	440	[12]
ICZ		1.66	5	440	
PU/CaO-25		14.5	65	450	This study
Manganese oxide coated zeolite	Cu(II)	7.9	62	183	[16]
Zeolite		1.15	5	440	[12]
ICZ		1.70	5	440	
PU/CaO-25		35.6	65	450	This study
Mucor rouxii	Ni(II)	0.36	10	1,800	[13]
Mollusk shells		0.26	105	20,790	[18]
Modified clay		12.9	22.6	100	[17]
PU/CaO-25		26.7	65	450	This study

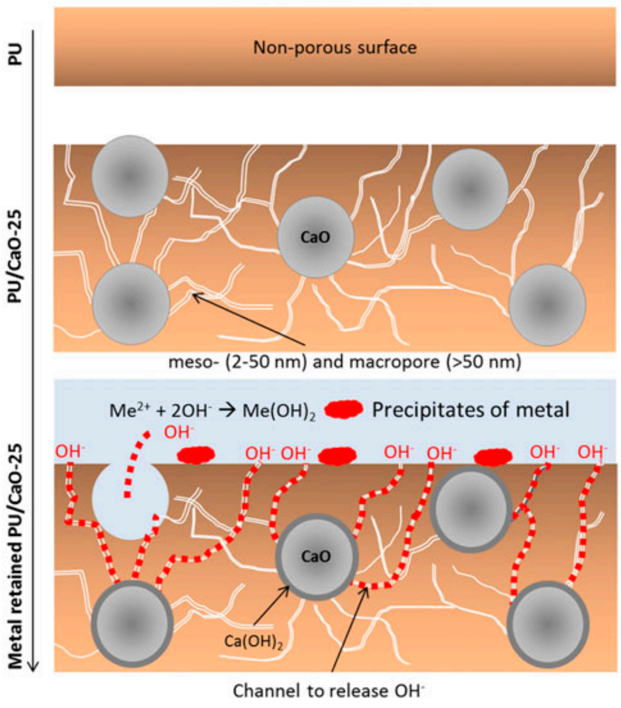

Fig. 9. Schematics of PU, PU/CaO-25 and metal removal mechanism.

has a compressive strength >0.15 MPa and a form density of 20–50 kg m^{-3} [39–42]. Thus, CaO addition enhanced the rigidity and density of the final PU product. Average HC of PU/CaO-25 tested and was 0.108 cm s^{-1}. Previous studies were reported HC of several sands [43–45] with sizes in the range 0.52–0.60 mm. Although PU/CaO-25 has a smaller average size (0.4 mm) than the referenced sands, it had an equivalent or higher HC. The HRT in the permeameter (74-mm ID × 160-mm L) was ~100 s, which was markedly shorter than those in column tests operated at 1.2 mL min^{-1} for 9-mL columns (225 s). The HC of the medium depends primarily on the pore size. Although larger pores conduct water more rapidly [46], the smooth surface might be another reason for the high HC as shown in the image of FESEM.

3.8. Treatment of simulated USRs by PU/CaO-25

Fig. 10 shows the column results of PU/CaO-25 with simulated USRs. The removal trends of most metals were similar at 0.5–1.2 mL min^{-1}, which are representative to slow and fast flow modes of USR. As the EBCT, they were 18 and 7.5 min, respectively. In particular, Cu(II) and Pb(II) concentrations started to increase gradually from 60 BVs, and a reached plateau at ~500 BVs although Cu(II) reached standard A at 1,100 BVs at 1.2 mL min^{-1}. Outlet concentrations of Zn (II) higher than the inlet level were detected at 1,000–1,100 BVs for 1.2 mL min^{-1} and 0.5 mL min^{-1},

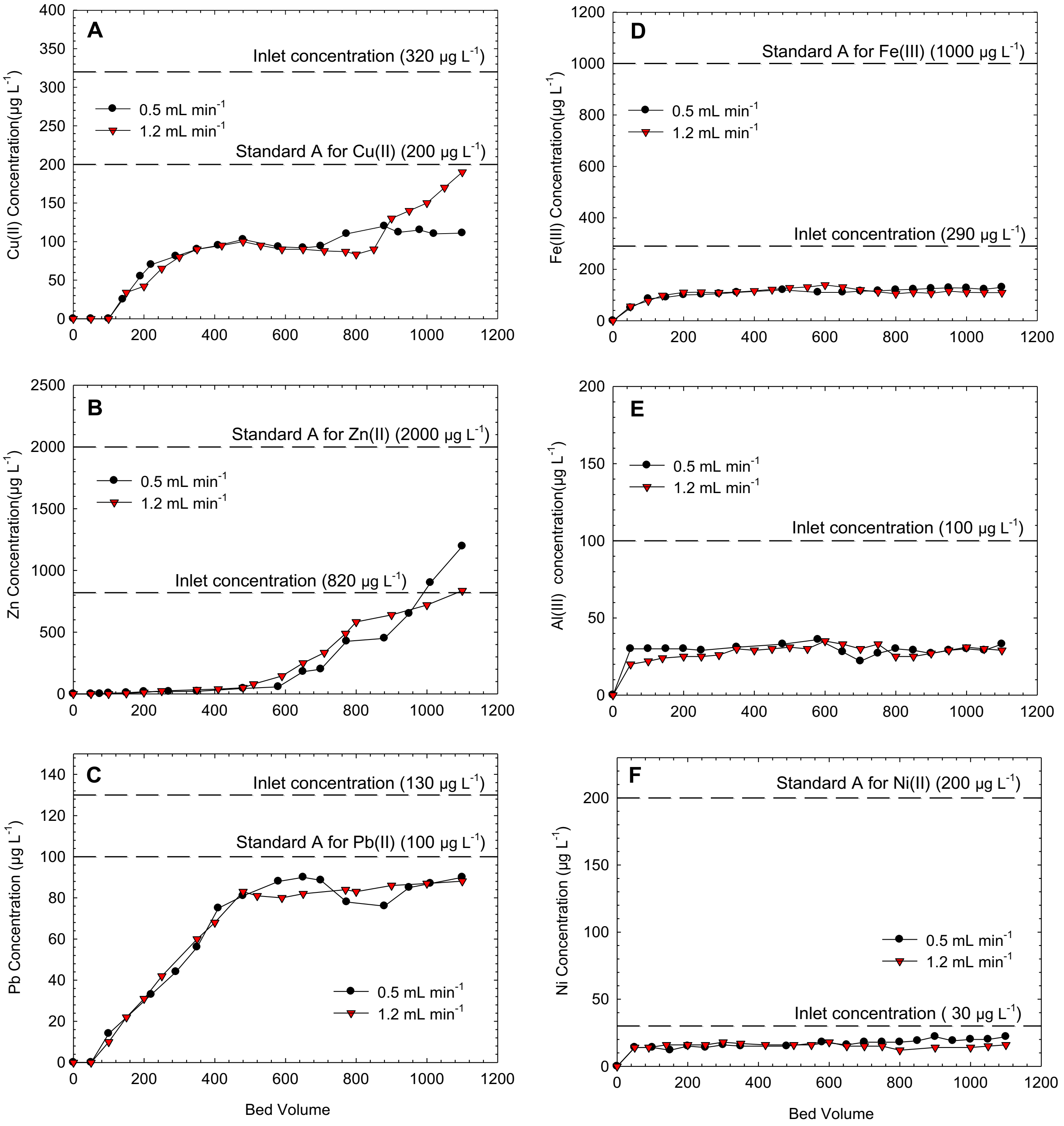

Fig. 10. Column results using simulated USR: outlet concentrations of (A) Cu(II), (B) Zn(II), (C) Pb(II), (D) Fe(III), (E) Al (III), and (F) Ni(II) according to bed volumes.

respectively. Fe(III), Al(III), and Ni(II) showed similar trends, with which all concentrations reached plateaus within 100 BVs and about 50–70% removal was obtained for 1,100 BVs. Table 4 shows the operational conditions of the column, inlet concentrations, and ARCs of heavy metals at 1,100 BVs.

Although there were different behaviors in heavy metal removal, the ARCs were strongly correlated with the inlet concentrations of the heavy metals. This result indicated the proposed removal mechanism in Section 3.3. Thus, OH^- continuously releases to precipitate Cu(II) without surface armoring of CaO.

Table 4
Column results using synthetic USR

Metals	Flowrate (mL min^{-1})	Inlet conc.		ARCs at 1,100 BVs		Standard A
		μg L^{-1}	μmol L^{-1}	μg g^{-1}	μmol g^{-1}	μg L^{-1}
Cu(II)	0.5	320	5	1,180	18.5	200
	1.2	320	5	1,146	17.9	
Zn(II)	0.5	820	12.4	2,787	42.6	2,000
	1.2	820	12.4	2,707	41.3	
Pb(II)	0.5	130	0.62	217	1.05	100
	1.2	130	0.62	367	1.77	
Al(III)	0.5	298	11	1,269	47	–
	1.2	298	11	1,348	50	
Fe(III)	0.5	141	2.52	173	3.09	1,000
	1.2	141	2.52	149.1	2.67	

Using the Medusa program, selective precipitations were interpreted based on the inlet concentrations of all heavy metals. Soluble and solid species of individual metals, terms of reactions, and equilibrium constants (log *K*) were defined for the USR conditions. Al(III) and Cu(II) were precipitated as $Al(OH)_3$ (cr) and $CuFe_2O_4$ (c), respectively, at pH 7–8, which was the pH range during column operation. Fe(III) existed as solids such as Fe_2O_3 (cr), $CuFe_2O_4$ (c), and $ZnFe_2O_4$ (c). Zn(II)/Pb(II) existed predominantly as ionic species—such as Zn^{2+}/Pb^{2+} and $ZnOH^+$/$PbOH^+$—at pH 7–7.5, and about 40% Zn(II) and 90% Pb(II) were transformed as $ZnFe_2O_4$/Zn$(OH)_2$ (c) and $Pb(OH)_2$ (c) at pH 8. Thus, as pH decreases, Zn(II) and Pb(II) become soluble species that can be removed by ion exchange. As shown in an earlier research [47], increase in ionic strength in the water has shown reduction in metal removal efficiency. Although, some authors well-explained the decrease in metal removal percentage caused by NaCl increase and the existence of Na+ ions for metal binding [48], it can be more clarified in terms of the different ionic species existing at different chloride concentrations. An increase in chloride concentration results in a decrease in the free divalent metal ions species and an increase in the corresponding chloro-complexes [47]. Based on the results above, PU/CaO-25 can be used to treat most heavy metals to below Standard A at 1,100 BVs. If we assume that 2,400-mm precipitation is collected annually in a 1,000-m^2 open space, the theoretical treatment volume and lifetime of a filter [1.5 m (ID) × 2 m (H), 4.4 m^3] containing PU/CaO-25 are 4,800 m^3 and ~2 years, respectively. When PU/CaO-25 is saturated, then we can easily recover it using a vacuum due to a low density.

4. Conclusions

To treat and reuse USR in an economical and effective manner, highly permeable rigid PU/CaO media were synthesized and tested in a fixed-bed column. All column data were predicted by use of BDST modeling. As special features, PU/CaO-25 had high rigidity (0.38 MPa) and permeability (0.108 cm s^{-1}), as well as relatively high removal capacities for heavy metals. The N_2 gas isotherm revealed that meso-and macropore structures developed as CaO was incorporated. This feature of PU/CaO helps to avoid armoring effect on CaO and resulted in continuous release of OH^-, which can successively precipitate heavy metals. Finally, precipitated metal ions were trapped in the available sites, as confirmed by FESEM/EDS and XRD analyses. In this study, column tests using simulated USR revealed that all heavy metals were remediated by PU/CaO-25 to below their regulation levels at ~1,100 BVs. Since metal precipitates are weakly trapped on the surface of PU, it is necessary to study on the optimum condition of regeneration. Based on its physicochemical properties and functionality, PU/CaO-25 can be used as an effective filter material for USR control and treatment with high capacities to remove heavy metals.

Acknowledgment

This project was funded by University of Malaya (UMRG, Sustainability Science, Project Number: RP010B-13SUS).

References

[1] M. Razzaghmanesh, S. Beecham, F. Kazemi, The growth and survival of plants in urban green roofs in a dry climate, Sci. Total Environ. 476–477 (2014) 288–297.

[2] D. Lemos, A.C. Dias, X. Gabarrell, L. Arroja, Environmental assessment of an urban water system, J. Cleaner Prod. 54 (2013) 157–165.

[3] F. Fu, Q. Wang, Removal of heavy metal ions from wastewaters: A review, J. Environ. Manage. 92(3) (2011) 407–418.

[4] E. Birlik, A. Ersöz, E. Açıkkalp, A. Denizli, R. Say, Cr (III)-imprinted polymeric beads: Sorption and preconcentration studies, J. Hazard. Mater. 140(1–2) (2007) 110–116.

[5] C.-Y. Cao, J. Qu, F. Wei, H. Liu, W.-G. Song, Superb adsorption capacity and mechanism of flowerlike magnesium oxide nanostructures for lead and cadmium ions, ACS Appl. Mater. Interfaces 4(8) (2012) 4283–4287.

[6] L. Westholm, E. Repo, M. Sillanpää, Filter materials for metal removal from mine drainage—A review, Environ. Sci. Pollut. Res. 21(15) (2014) 9109–9128.

[7] K. Huang, Y. Xiu, H. Zhu, Selective removal of Cr(VI) from aqueous solution by adsorption on mangosteen peel, Environ. Sci. Pollut. Res. 20(9) (2013) 5930–5938.

[8] K. Huang, H. Zhu, Removal of Pb^{2+} from aqueous solution by adsorption on chemically modified muskmelon peel, Environ. Sci. Pollut. Res. 20(7) (2013) 4424–4434.

[9] M. Sprynskyy, T. Kowalkowski, H. Tutu, L.M. Cozmuta, E.M. Cukrowska, B. Buszewski, The adsorption properties of agricultural and forest soils towards Heavy metal ions (Ni, Cu, Zn, and Cd), Soil Sediment Contam. An Int. J. 20(1) (2010) 12–29.

[10] J. Hizal, E. Tutem, K. Guclu, M. Hugul, S. Ayhan, R. Apak, F. Kilinckale, Heavy metal removal from water by red mud and coal fly ash: An integrated adsorption–solidification/stabilization process, Desalin. Water Treat. 51(37–39) (2013) 7181–7193.

[11] S. Bekkouche, S. Baup, M. Bouhelassa, S. Molina-Boisseau, C. Petrier, Competitive adsorption of phenol and heavy metal ions onto titanium dioxide (Dugussa P25), Desalin. Water Treat. 37(1–3) (2012) 364–372.

[12] T.C. Nguyen, P. Loganathan, T.V. Nguyen, S. Vigneswaran, J. Kandasamy, R. Naidu, Simultaneous adsorption of Cd, Cr, Cu, Pb, and Zn by an iron-coated Australian zeolite in batch and fixed-bed column studies, Chem. Eng. J. 270 (2015) 393–404.

[13] G. Yan, T. Viraraghavan, Heavy metal removal in a biosorption column by immobilized M. rouxii biomass, Bioresour. Technol. 78(3) (2001) 243–249.

[14] E.I. Unuabonah, M.I. El-Khaiary, B.I. Olu-Owolabi, K.O. Adebowale, Predicting the dynamics and performance of a polymer–clay based composite in a fixed bed system for the removal of lead (II) ion, Chem. Eng. Res. Des. 90(8) (2012) 1105–1115.

[15] B. Salamatinia, A.H. Kamaruddin, A.Z. Abdullah, Modeling of the continuous copper and zinc removal by sorption onto sodium hydroxide-modified oil palm frond in a fixed-bed column, Chem. Eng. J. 145(2) (2008) 259–266.

[16] R. Han, W. Zou, H. Li, Y. Li, J. Shi, Copper(II) and lead(II) removal from aqueous solution in fixed-bed columns by manganese oxide coated zeolite, J. Hazard. Mater. 137(2) (2006) 934–942.

[17] T. Vengris, R. Binkiene, A. Sveikauskaite, Nickel, copper and zinc removal from waste water by a modified clay sorbent, Appl. Clay Sci. 18(3–4) (2001) 183–190.

[18] C. Li, P. Champagne, Fixed-bed column study for the removal of cadmium (II) and nickel (II) ions from aqueous solutions using peat and mollusk shells, J. .Hazard. Mater. 171(1–3) (2009) 872–878.

[19] G. Yang, H. Han, C. Du, Z. Luo, Y. Wang, Facile synthesis of melamine-based porous polymer networks and their application for removal of aqueous mercury ions, Polymer 51(26) (2010) 6193–6202.

[20] H. Choi, N.C. Woo, M. Jang, F.S. Cannon, S.A. Snyder, Magnesium oxide impregnated polyurethane to remove high levels of manganese cations from water, Sep. Purif. Technol. 136 (2014) 184–189.

[21] E. Uğuzdoğan, E.B. Denkbaş, E. Öztürk, S.A. Tuncel, O.S. Kabasakal, Preparation and characterization of polyethyleneglycolmethacrylate (PEGMA)-co-vinylimidazole (VI) microspheres to use in heavy metal removal, J. Hazard. Mater. 162(2–3) (2009) 1073–1080.

[22] V. Singh, S. Pandey, S.K. Singh, R. Sanghi, Removal of cadmium from aqueous solutions by adsorption using poly(acrylamide) modified guar gum–silica nanocomposites, Sep. Purif. Technol. 67(3) (2009) 251–261.

[23] R. Kanthapazham, C. Ayyavu, D. Mahendiradas, Removal of Pb^{2+}, Ni^{2+} and Cd^{2+} ions in aqueous media using functionalized MWCNT wrapped polypyrrole nanocomposite, Desalin. Water Treat. (2015) 1–15.

[24] S. Hora, G. Simu, L. Bugariu, A. Popa, R. Rad, Azo direct dye immobilized onto copolymer (styrene DVB functionalized with quaternary phosphonium groups) for removal of heavy metal ions, Mol. Cryst. Liq. Cryst. 416(1) (2004) 137–144.

[25] S. Netpradit, P. Thiravetyan, S. Towprayoon, Evaluation of metal hydroxide sludge for reactive dye adsorption in a fixed-bed column system, Water Res. 38(1) (2004) 71–78.

[26] U.M. Joshi, R. Balasubramanian, Characteristics and environmental mobility of trace elements in urban runoff, Chemosphere 80(3) (2010) 310–318.

[27] C. Ong, S. Ibrahim, B. Sen Gupta, A survey of tap water quality in Kuala Lumpur, Urban Water J. 4(1) (2007) 29–41.

[28] D. Charumathi, N. Das, Packed bed column studies for the removal of synthetic dyes from textile wastewater using immobilised dead C. tropicalis, Desalination 285 (2012) 22–30.

[29] K. Vijayaraghavan, J. Jegan, K. Palanivelu, M. Velan, Biosorption of cobalt(II) and nickel(II) by seaweeds: Batch and column studies, Sep. Purif. Technol. 44(1) (2005) 53–59.

[30] Z. Zulfadhly, M. Mashitah, S. Bhatia, Heavy metals removal in fixed-bed column by the macro fungus pycnoporus sanguineus, Environ. Pollut. 112(3) (2001) 463–470.

[31] S.H. Hasan, D. Ranjan, M. Talat, Agro-industrial waste 'wheat bran' for the biosorptive remediation of selenium through continuous up-flow fixed-bed column, J. Hazard. Mater. 181(1–3) (2010) 1134–1142.

[32] S. Mohan, G. Sreelakshmi, Fixed bed column study for heavy metal removal using phosphate treated rice husk, J. Hazard. Mater. 153(1–2) (2008) 75–82.

[33] Y.S. Al-Degs, M.I. El-bBarghouthi, A.A. Issa, M.A. Khraisheh, G.M. Walker, Sorption of Zn(II), Pb(II), and Co(II) using natural sorbents: Equilibrium and kinetic studies, Water Res. 40(14) (2006) 2645–2658.

[34] B.M.W.P.K. Amarasinghe, R.A. Williams, Tea waste as a low cost adsorbent for the removal of Cu and Pb from wastewater, Chem. Eng. J. 132(1–3) (2007) 299–309.

[35] Ö. Yavuz, Y. Altunkaynak, F. Güzel, Removal of copper, nickel, cobalt and manganese from aqueous solution by kaolinite, Water Res. 37(4) (2003) 948–952.

[36] B. Yu, Y. Zhang, A. Shukla, S.S. Shukla, K.L. Dorris, The removal of heavy metals from aqueous solutions by sawdust adsorption—Removal of lead and comparison of its adsorption with copper, J. Hazard. Mater. 84(1) (2001) 83–94.

[37] C. Hasfalina, R. Maryam, C. Luqman, M. Rashid, Adsorption of copper (II) from aqueous medium in fixed-bed column By kenaf fibres, APCBEE Procedia 3 (2012) 255–263.

[38] B.K. Das, K.N. Das, Adsorption-desorption of zinc as influenced by fly ash in inceptisols of Assam, Commun. Soil Sci. Plant Anal. 46(6) (2015) 800–818.

[39] G. Oertel, L. Abele, Polyurethane Handbook: Chemistry, Raw Materials, Processing, Application, Properties, Hanser Publishers. Distributed in USA by Scientific and Technical Books, Macmillan, 1985.

[40] T. Widya, C.W. Macosko, Nanoclay-modified rigid polyurethane foam, J. Macromol. Sci. Part B Phys. 44 (6) (2005) 897–908.

[41] M. Szycher, Szycher's Handbook of Polyurethanes, CRC press, Florida, FL, 1999.

[42] S.-T. Lee, N.S. Ramesh, Polymeric Foams, CRC press, Florida, FL, 2004.

[43] K.M. Smits, V.V. Ngo, A. Cihan, T. Sakaki, T.H. Illangasekare, An evaluation of models of bare soil evaporation formulated with different land surface boundary conditions and assumptions, Water Resour. Res. 48(12) (2012) 125–126.

[44] D. Seifert, P. Engesgaard, Sand box experiments with bioclogging of porous media: Hydraulic conductivity reductions, J. Contam. Hydrol. 136–137 (2012) 1–9.

[45] C.-H. Hsieh, A.P. Davis, Evaluation and optimization of bioretention media for treatment of urban storm water runoff, J. Environ. Eng. 131(11) (2005) 1521–1531.

[46] D. Hillel, Environmental soil physics: Fundamentals, applications, and environmental considerations, Academic press, Massachusetts, MA, 1998.

[47] F. Ge, M.-M. Li, H. Ye, B.-X. Zhao, Effective removal of heavy metal ions Cd^{2+}, Zn^{2+}, Pb^{2+}, Cu^{2+} from aqueous solution by polymer-modified magnetic nanoparticles, J. Hazard. Mater. 211–212 (2012) 366–372.

[48] N. Fiol, I. Villaescusa, M. Martínez, N. Miralles, J. Poch, J. Serarols, Sorption of Pb(II), Ni(II), Cu(II) and Cd(II) from aqueous solution by olive stone waste, Sep. Purif. Technol. 50(1) (2006) 132–140.